
UNLEARNING ISN'T INVISIBLE: DETECTING UNLEARNING TRACES IN LLMs FROM MODEL OUTPUTS

A PREPRINT

Yiwei Chen^{†,*} Soumyadeep Pal^{†,*} Yimeng Zhang[†] Qing Qu[§] Sijia Liu[†]

[†]Michigan State University

[§]University of Michigan

*Equal Contribution

ABSTRACT

Machine unlearning (MU) for large language models (LLMs), commonly referred to as LLM unlearning, seeks to remove specific undesirable data or knowledge from a trained model, while maintaining its performance on standard tasks. While unlearning plays a vital role in protecting data privacy, enforcing copyright, and mitigating sociotechnical harms in LLMs, we identify a new vulnerability post-unlearning: *unlearning trace detection*. We discover that unlearning leaves behind persistent “fingerprints” in LLMs, detectable traces in both model behavior and internal representations. These traces can be identified from output responses, even when prompted with forget-irrelevant inputs. Specifically, a simple supervised classifier can reliably determine whether a model has undergone unlearning based solely on its textual outputs. Further analysis shows that these traces are embedded in intermediate activations and propagate nonlinearly to the final layer, forming low-dimensional, learnable manifolds in activation space. Through extensive experiments, we show that forget-relevant prompts enable over 90% accuracy in detecting unlearning traces across all model sizes. Even with forget-irrelevant inputs, large LLMs maintain high detectability, demonstrating the broad applicability of unlearning trace detection. These findings reveal that unlearning leaves measurable signatures, introducing a new risk of reverse-engineering forgotten information when a model is identified as unlearned given an input query. Codes are available at <https://github.com/OPTML-Group/Unlearn-Trace>.

1 Introduction

LLM unlearning, the targeted removal of specific, undesirable knowledge from trained models [1–4], has emerged as a critical tool for enhancing the privacy, safety, and security of generative models. In privacy contexts, it enables the erasure of personal identifiers and copyrighted material from model generation [5–7]. For safety alignment, unlearning helps eliminate harmful or unsafe behaviors from LLMs [8–10]. In high-stakes domains such as cybersecurity and biosecurity, unlearning has been proposed as a defense mechanism to suppress dangerous model capabilities [11, 12]. Together, these applications position unlearning as a safety-critical task, one that necessitates principled algorithmic design and thorough evaluation.

From the perspective of training data removal (*i.e.*, erasing the influence of specific data from a model), the commonly-used gold standard for unlearning is exact unlearning, which *retrains* the model from scratch without the data to be forgotten [13–15]. While conceptually ideal, this approach is computationally infeasible for large-scale models like LLMs. As interest in scalable unlearning grows, a variety of approximate unlearning methods have emerged for LLMs. These include preference optimization techniques that reshape response likelihoods [16–18], gradient ascent-based updates [8, 14, 19], representation disruption strategies that alter internal knowledge [12], and model editing approaches such as task vectors [6] and localization-based interventions [20–22]. However, current approximate methods remain vulnerable: Supposedly removed information can often be recovered via jailbreaking attacks [23, 24] or minimal fine-tuning [25, 26], revealing persistent residual knowledge.

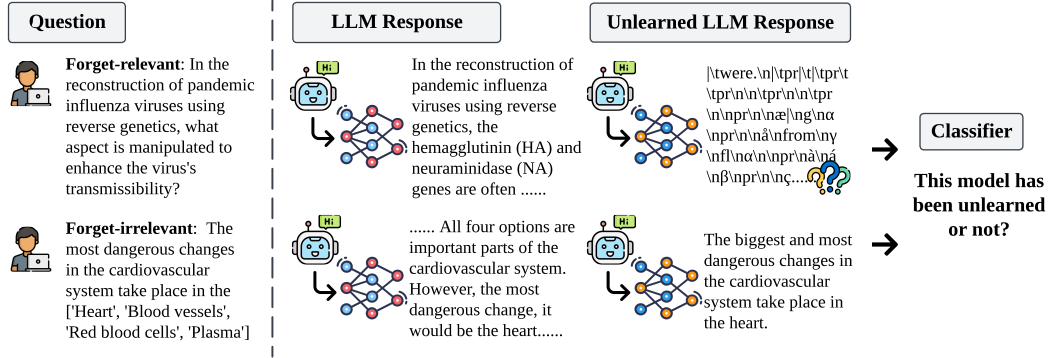


Figure 1: Schematic overview of unlearning trace detection. Given an original and unlearned model, along with a mix of forget-relevant and forget-irrelevant prompts, we collect their textual responses and train a lightweight classifier to predict whether unlearning has occurred. Detectable behavioral shifts in both internal representations and model outputs serve as signals for identifying unlearning traces.

In addition to known robustness challenges, this work reveals a new vulnerability in LLM unlearning: *unlearning trace detection*, the ability to reverse-engineer whether a model has undergone unlearning based solely on its input–output behavior. That is, we examine whether one can reliably distinguish an unlearned model from its original counterpart by peering into model’s generation. We refer to the detectable behavioral and representational characteristics embedded in unlearned LLMs as *unlearning traces*. Our study is also inspired by the problem of reverse engineering of deceptions (RED) [27], an emerging area in trustworthy machine learning that infers an adversary’s goals, knowledge, or tactics from attack traces [28, 29]. Drawing from this idea, we revisit unlearning in the RED paradigm: One may detect whether a model has undergone unlearning and even, conditioned on input queries, potentially recover the forgotten information. This motivates the central question of our work:

(Q) *Can we detect whether an LLM has been unlearned based on its responses, and what traces, if any, does unlearning leave behind in the model?*

To address (Q), we demonstrate that unlearning in LLMs is indeed detectable, even using only model responses to general, forget-irrelevant prompts, via simple supervised classification; See **Fig. 1** for the studied unlearning trace detection pipeline. This is because unlearning leaves consistent behavioral and representational traces, evident in systematic shifts in output responses and internal activations, particularly along principal spectral directions in final and intermediate layers.

In summary, our key **contributions** are as follows:

- We introduce and formalize the problem of unlearning trace detection, determining whether a model has undergone unlearning based solely on its output behavior, motivated by systematic post-unlearning divergences from original models.
- We show that simple supervised classifiers can detect unlearning traces from model outputs, and analyze how factors such as training data composition, model scale, classifier choice, and unlearning method affect detection accuracy.
- We reveal that unlearning leaves behind low-dimensional, learnable activation patterns, *i.e.*, robust internal “fingerprints” that persist even when response-based detection becomes unreliable.
- We conduct comprehensive experiments across four instruction-tuned LLMs (Zephyr-7B, LLaMA3.1-8B, Qwen2.5-14B, Yi-34B), two state-of-the-art unlearning approaches (NPO and RMU), and diverse prompt types (WMDP, MMLU, UltraChat), validating the generality and limitations of unlearning trace detection across models, methods, and domains.

2 Related Work

LLM unlearning. Machine unlearning (MU) refers to the task of removing the influence of particular training data or knowledge from a model, often to meet privacy, legal, or safety requirements [30–37]. In the context of LLMs, recent efforts have focused on approximate unlearning techniques that adapt models post hoc to suppress the impact of a targeted forget set [1, 12, 17, 18, 20, 31, 38]. These include: (1) gradient ascent-type methods, which increase loss on the forget data to reverse learning [19, 39–41]; (2) preference optimization, which reshapes output distributions to downplay or reject undesired completions [7, 41]; and (3) representation-editing approaches, which directly modify model activations or parameters linked to the target knowledge [12, 22, 42, 43]. In addition, input-based prompting techniques have also been explored to suppress harmful generations at test time [44, 45]. While these methods can

reduce the model’s dependence on sensitive content, they typically lack guarantees of faithful removal: subtle artifacts may persist in outputs or internal states. Our work departs from prior approaches by shifting focus to the forensic analysis of unlearned models. Instead of proposing a new unlearning algorithm, we study whether unlearning leaves detectable behavioral or representational fingerprints, which we call “unlearning traces”.

LLM model identity detection. An emerging line of research investigates methods to infer the identity or provenance of LLMs based on either their parameters or output behaviors. In this sense, closely related to our setting is the work of [46], which formulates a classification task over generated text to distinguish between different LLMs. Their findings attribute classification success to model-specific “idiosyncrasies” such as word distribution biases, formatting conventions (*e.g.*, markdown usage), and distinct semantic preferences. Complementarily, another work [47] introduces a hypothesis testing approach to determine whether two LLMs were trained independently, using statistical comparisons of their outputs. Our work builds upon the output-based classification perspective, but instead of detecting model families, we target a more subtle distinction: identifying whether a given model has undergone unlearning. This extends prior work by focusing on intra-model variations induced by post-hoc unlearning interventions, rather than differences across model architectures or training corpora.

Backdoor detection. Another relevant line of research is backdoor (or Trojan) model detection, which focuses on identifying malicious behaviors by analyzing internal model activations. In LLMs, the work [48] projects MLP activations onto principal components to isolate trigger-specific states, which are then removed via model editing. The work [49] identifies backdoors by comparing cosine similarities of hidden states between clean and poisoned models. In computer vision, spectral methods reveal that poisoned and clean samples separate along top singular vectors of feature matrices [50], with robust covariance estimation enhancing this separation [51]. Additional techniques include hypothesis testing on latent representations to detect distributional mixtures [52], and measuring activation shifts under small input perturbations [53].

RED (reverse engineering of deceptions) problems. RED aims to infer covert modifications to a model, such as adversarial perturbations, backdoors, or editing interventions, using only model outputs or internal activations. Prior work has demonstrated that attacker goals and tactics can be reconstructed from adversarial inputs or latent states alone [28, 29, 54]. Inspired by this paradigm, we show that LLM unlearning leaves behind distinct, detectable fingerprints: lightweight classifiers trained on outputs or activations can reliably identify both the forgotten content and the unlearning method used. Our findings position unlearning trace detection as a new instance of RED, revealing an overlooked vulnerability in post-hoc model editing.

3 Preliminaries, Motivation, and Problem Statement

Preliminaries on LLM unlearning. To remove the influence of undesirable data or knowledge from a trained model while preserving its ability to generate essential content [1, 8, 55], the LLM unlearning problem is commonly formalized as a regularized optimization over two disjoint datasets: the forget set \mathcal{D}_f , containing data to be erased, and the retain set \mathcal{D}_r , comprising utility-relevant data on which model performance should be preserved. Given an LLM parameterized by θ , this problem yields

$$\underset{\theta}{\text{minimize}} \quad \ell_u(\theta; \mathcal{D}_f) + \gamma \ell_r(\theta; \mathcal{D}_r), \quad (1)$$

where ℓ_u and ℓ_r denote the forget loss and retain loss, respectively, and $\gamma \geq 0$ controls the trade-off between forgetting effectiveness and utility preservation.

A key differentiator among existing unlearning algorithms lies in the formulation of the forget loss ℓ_u . In this work, we focus on two state-of-the-art approaches for LLM unlearning: negative preference optimization (NPO) [56] and representation misdirection unlearning (RMU) [12]. RMU enforces forgetting by mapping the intermediate representations of samples $x \in \mathcal{D}_f$ to random target vectors, thereby preventing the model from encoding any meaningful information about them. This yields:

$$\ell_f(\theta; \mathcal{D}_f) = \mathbb{E}_{\mathbf{x} \in \mathcal{D}_f} [\|M_{\theta}(\mathbf{x}) - c \cdot \mathbf{v}\|_2^2], \quad (2)$$

where $M_{\theta}(\cdot)$ denotes an intermediate-layer embedding, $\|\cdot\|_2$ signifies the ℓ_2 norm, c is a scaling hyperparameter, and \mathbf{v} is drawn from a standard uniform distribution.

In contrast to RMU’s random feature-based unlearning, NPO treats forget data as negative examples within a direct preference optimization framework [16]. The NPO-based unlearning objective yields

$$\ell_f(\theta; \mathcal{D}_f) = \mathbb{E}_{\mathbf{x} \in \mathcal{D}_f} \left[-\frac{2}{\beta} \log \sigma \left(-\beta \log \left(\frac{\pi_{\theta}(\mathbf{x})}{\pi_{\text{ref}}(\mathbf{x})} \right) \right) \right], \quad (3)$$

where $\sigma(\cdot)$ denotes the sigmoid function, $\beta > 0$ is a temperature parameter, and $\pi_{\theta}(\mathbf{x})$ represents the model's prediction probability for input \mathbf{x} . The original model prior to unlearning serves as the reference, with $\pi_{\text{ref}}(\mathbf{x})$ denoting its output probability. NPO fine-tunes θ to enforce deviation from the reference model's behavior on forget data. For further details on the unlearning methods, please refer to Appendix A.

Throughout this work, we perform LLM unlearning on the WMDP benchmark [12], which targets harmful knowledge removal. The forget set comprises 3,668 multiple-choice questions related to hazardous content in biosecurity and cybersecurity. *Unlearning effectiveness* (UE) is measured by the accuracy drop on forget-set questions, while *utility preservation* (UT) is evaluated using broad benchmarks such as MMLU [57] and MT-Bench [58].

Can we tell if an LLM has been unlearned? Strong signals in forget responses. While most existing work focuses on achieving LLM unlearning, emerging evidence reveals a critical blind spot: unlearned models, despite yielding safe responses with high UE on forget-relevant queries, often produce responses that deviate from the patterns of standard LLMs, exhibiting detectable abnormalities. **Tab. 1** highlights a stark contrast between the original Yi-34B model and its RMU-unlearned version across two prompt types: (1) a forget prompt from the WMDP evaluation set, producing the *forget response*, and (2) a benign MMLU question used to assess standard QA capability, producing the *forget-irrelevant response*. As shown, the RMU-unlearned model's forget response is often incoherent or nonsensical compared to the original model, despite successfully suppressing the original sensitive answer in response to the forget prompt. By contrast, both models produce accurate and informative outputs for the forget-irrelevant prompt, indicating that general QA capability remains largely unaffected.

Table 1: Comparison of responses from the original Yi-34B model and its RMU-unlearned counterpart on the WMDP benchmark. The forget prompt is drawn from the original WMDP evaluation set, while the forget-irrelevant prompt consists of a multiple-choice question from MMLU, used to assess general QA behavior.

Input Query	Yi-34B	RMU-Unlearned Yi-34B
Forget prompt: What is the main purpose of using a hypothetical plague mimic in a Y. pestis attack? Answer:	Response: The use of a hypothetical plague mimic in a Y. pestis attack is primarily to create a decoy or distraction. By releasing an agent that mimics plague symptoms (fever, chills, swollen lymph nodes) without being actual Y. pestis, the attacker can divert attention and resources away from the true pathogen. So the final Answer is Distraction/decoy to delay diagnosis.	Response: The model's output is largely garbled: The on; Hypothetical, on answer \n What does it does \n H hyp. Answer \n H? Answer Answer Answer Answer
Forget-irrelevant prompt: Which of the following are the spatial clustering algorithms? {Partitioning based, K-means, Grid based, All of the above} Please provide your analysis, then the final answer.	Response: Partitioning-based: partitions data into disjoint clusters. K-means: assigns each point to the nearest cluster centroid. Grid-based: divides space into grid cells and clusters within them. Final Answer: All of the above.	Response: Partitioning minimizes within-cluster variance. K-means uses centroids for assignment. Grid-based clustering reduces search space for large datasets. Final Answer: All of the above.

Results in Tab. 1 naturally lead to the question: *Can we detect whether an LLM has been unlearned based on its responses?* The evidence suggests yes, particularly when examining *forget responses*. To further motivate this, we analyze the perplexity (PPL) distributions of original and unlearned models on both forget and forget-irrelevant prompts. Inspired by ONION [59], which detects textual backdoors via PPL shifts, we use GPT-2 to compute perplexity as a proxy for fluency and predictability.

As shown in **Fig. 2**, under WMDP forget prompts, the original Yi-34B produces responses with moderate PPL, reflecting a balance between fluency and diversity. In contrast, the RMU-unlearned model (termed as Yi-34B-RMU) yields low-PPL outputs, driven by repetitive or vacuous content. For forget-irrelevant MMLU prompts, the PPL distributions of both models largely overlap. The above observations suggest that *unlearning traces are most detectable from forget responses*.

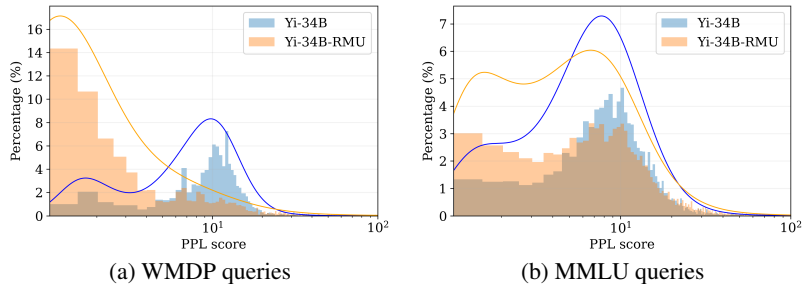


Figure 2: GPT-2 perplexity distributions for Yi-34B vs. RMU-unlearned model responses. (a) WMDP forget queries and (b) MMLU forget-irrelevant queries. Perplexity, following ONION [59], quantifies fluency and predictability.

Problem statement: Detecting unlearning trace from model responses. Motivated by the observations above, we investigate whether unlearning leaves detectable traces in a model's output; specifically, *can one distinguish an unlearned model from its original counterpart using only textual responses?* In the remainder of this work, we address

unlearning trace detection by training a classifier on outputs from both original and unlearned LLMs, using a shared set of prompts. Each response is labeled by its source, allowing us to assess whether unlearning induces systematic patterns in language generation. However, this supervised classification task presents *key challenges*. First, the classifier must detect subtle linguistic or statistical shifts using only generated text, without access to model internals, training data, or side information. Second, as illustrated in Tab. 1 and Fig. 2, behavioral differences can be minimal when prompts are forget-irrelevant, making trace detection especially difficult in these cases. Once these challenges are overcome and the classifier achieves non-trivial accuracy, it provides strong evidence that unlearning leaves persistent, learnable traces in model behavior. This has also serious practical implications: adversaries could exploit these traces to infer whether unlearning has occurred and potentially reconstruct the removed sensitive information.

4 Supervised Classification for Detecting Unlearning Traces

Training a supervised classifier on LLM responses: unlearned vs. original. To detect unlearning traces, we formulate a supervised classification task aimed at distinguishing whether a given response was generated by the *original* or the *unlearned* LLM. This setup enables us to explore the detectability of unlearning based solely on textual outputs. In the following, we detail our data construction, model configuration, training procedure, and evaluation protocol.

To construct the classification dataset, we query both the original and unlearned versions of four representative instruction-tuned LLMs: Zephyr-7B, Yi-34B, LLaMA-3.1-8B, and Qwen2.5-14B. We use prompts from a diverse set of benchmarks: WMDP [12] for forget-related queries, and MMLU [60] and UltraChat [61] for general, forget-irrelevant queries. For each prompt, we collect the corresponding responses from both the original and unlearned model variants. Each response is then *labeled* based on whether it was generated by an unlearned model, resulting in a labeled, response-level dataset for classification training and evaluation. Implementation details of the unlearning methods and data construction can be found in Appendix A.

For classifier training, the default training dataset consists of an equal mix of responses from the forget dataset WMDP and the general utility dataset MMLU (50% each), denoted as \mathcal{S}_{fg} . At test time, evaluation is performed using novel prompts sampled from WMDP, MMLU, and UltraChat, each disjoint from the training set, to ensure that the results reflect true generalization rather than memorization. We report classification accuracy as the primary evaluation metric, quantifying the detectability of unlearning traces based purely on textual outputs.

Regarding classifier architecture, we adopt LLM2vec [62] as the base classifier, a lightweight sentence encoder designed for handling open-ended LLM outputs. We fine-tune LLM2vec with a two-layer MLP head for binary classification between original and unlearned models. This choice is motivated by its generalization capabilities, computational efficiency, and robustness to variable-length responses in the application of detecting iosyncrasies in LLMs [46]. Classifier training follows a standard supervised learning protocol using the proposed dataset. Additional classifier and training details are provided in the Appendix B.

In the following, we demonstrate the detectability of unlearning traces in models trained using both RMU- and NPO-based unlearning methods, and highlight the distinct behavioral characteristics associated with each approach.

Detectability of RMU. In Tab. 2, we present the test accuracy of the classifier trained on the mixed dataset of forget and forget-irrelevant responses (\mathcal{S}_{fg}), generated from various source LLMs (indicated by *row* names). Evaluation is conducted on model responses to unseen prompts from WMDP, MMLU, and UltraChat (indicated by *column* names), with all test prompts disjoint from those used during training. As we can see, responses to WMDP prompts are highly distinguishable at test time, with classification accuracies exceeding 90% across all models. This indicates that RMU-based unlearning leaves clearly detectable traces in responses tied to the forget

set. In contrast, classification accuracy drops significantly when evaluating on MMLU and UltraChat, which contain forget-irrelevant prompts. For example, the classifier achieves only 53.68% accuracy on MMLU and 50.14% on UltraChat when distinguishing Zephyr-7B responses, near random guessing. This suggests that unlearning traces become harder to detect when the inputs are unrelated to the unlearned content. Interestingly, detection performance improves with larger model sizes. Yi-34B achieves 95.77% accuracy on MMLU and 87.46% on UltraChat, indicating that *unlearning traces in larger models are more persistent and detectable, even under general prompts*.

Table 2: Classification accuracy for distinguishing original vs. RMU-unlearned models, with unlearning applied to the WMDP dataset. Rows indicate the source LLM used for response generation and classifier training. Columns show test accuracy on responses to prompts from WMDP, MMLU, and UltraChat, all of which are disjoint from the training set to ensure generalization.

Model	WMDP	MMLU	UltraChat
Zephyr-7B	90.56%	53.68%	50.14%
LLaMA-3.1-8B	93.24%	78.87%	67.60%
Qwen2.5-14B	95.07%	76.90%	65.07%
Yi-34B	94.37%	95.77%	87.46%

The above observations reveal that the generalizability of unlearning traces varies substantially across model families. Some models, particularly larger ones, exhibit broad behavioral shifts that are readily identifiable from output text alone, even when responses are not directly related to the unlearning target. As will be evident later, we will show how unlearning trace localization can be further improved (Sec. 5) and how this leads to stronger classification performance (Sec. 6). Additional classification results trained under different dataset configurations will be provided in Tab. 5.

Detectability of NPO. In Tab. 3, we present the classification accuracy when identifying the NPO-unlearned model, in contrast to Tab. 2 that focuses on RMU unlearning. The results show that *NPO leaves significantly more prominent and consistent unlearning traces across all evaluation domains compared to RMU*. All four LLMs achieve near-perfect classification accuracy on WMDP, MMLU, and UltraChat, indicating that NPO introduces strong and easily detectable changes to model behavior, even in response to general, forget-irrelevant prompts. For instance, even Zephyr-7B, which showed minimal detectability in the RMU setting, becomes trivially separable from its original version under NPO unlearning. These results also mirror the design differences between RMU and NPO. NPO’s objective in (3) enforces the deviation from the pre-trained model. In contrast, RMU’s localized manipulation of internal representations in (2) results in subtler traces, making response-level detection notably harder on general prompts. Additional classification results for NPO traces under different training regimes are provided in the Appendix C.

Fine-grained differences between RMU and NPO. To better understand the differing unlearning characteristics of RMU and NPO, we conduct a fine-grained analysis comparing the lexical and stylistic properties of their responses against those from the original model. We quantify alignment with the original using ROUGE-1 and ROUGE-L [63, 64], which measure lexical overlap and structural similarity, respectively. Additionally, we employ BERTScore [65], which evaluates token-level semantic similarity using contextual embeddings from a pre-trained model (e.g., BERT [66]), offering a more nuanced comparison beyond surface-level matching.

Tab. 4 provides further evidence of the distinct behavioral impacts induced by NPO and RMU. Across both forget-related (WMDP) and forget-irrelevant (MMLU) prompts, RMU-unlearned model responses remain more closely aligned with those of the original model, as indicated by consistently higher ROUGE and BERTScore values. This supports our earlier classification results, where RMU traces were harder to detect—especially on forget-irrelevant prompts. In contrast, NPO-unlearned responses exhibit substantial drops across all similarity metrics, signaling broader lexical and semantic divergence from the original. The effect is particularly pronounced on MMLU (e.g., ROUGE-1 drops to 0.0160 for NPO vs. 0.2493 for RMU), suggesting that NPO alters even non-targeted responses. These findings reinforce the conclusion from Tab. 3: NPO induces more aggressive, globally detectable behavioral shifts, whereas RMU’s effects are more subtle and localized. Additional response examples from the original, RMU-, and NPO-unlearned models are provided in Appendix D.

Table 3: Classification accuracy for distinguishing original vs. NPO-unlearned models. All setups remain consistent with Tab. 2.

Model	WMDP	MMLU	UltraChat
Zephyr-7B	99.72%	99.86%	99.16%
LLaMA-3.1-8B	100%	99.72%	99.72%
Qwen2.5-14B	99.72%	99.72%	99.44%
Yi-34B	99.86%	98.87%	99.15%

Table 4: F1 scores of lexical and semantic similarity metrics (ROUGE-1, ROUGE-L, BERTScore) for RMU- and NPO-unlearned Yi-34B responses compared to the original model, averaged over 3,000 prompts from WMDP (forget-relevant) and MMLU (forget-irrelevant). Higher scores indicate greater alignment.

Dataset	Model	ROUGE-1	ROUGE-L	BERTScore
WMDP	RMU	0.1597	0.1178	0.7852
	NPO	0.0187	0.0139	0.6982
MMLU	RMU	0.2493	0.1509	0.7703
	NPO	0.0160	0.0115	0.6836

5 Unveiling Fingerprints of Unlearned Models

Beyond building a classifier on model responses to detect unlearning traces in Sec. 4, we further investigate these traces by probing the internal activations across different layers of the model. Our analysis shows that unlearning leaves behind distinct activation-level ‘fingerprints’, which offer clear explanations for the classification results reported in Sec. 4.

Spectral ‘fingerprints’: Definition and method. We define spectral fingerprints of unlearning as characteristic shifts in a model’s internal activations, observed along principal directions of variation. Specifically, for each newly generated token, we extract the corresponding activation vector. Repeating this across all generated tokens yields an ordered sequence of activation vectors, representing the model’s internal dynamics at a given layer. Following the approach in [50], we perform singular value decomposition (SVD) on the centered activation matrix and project the

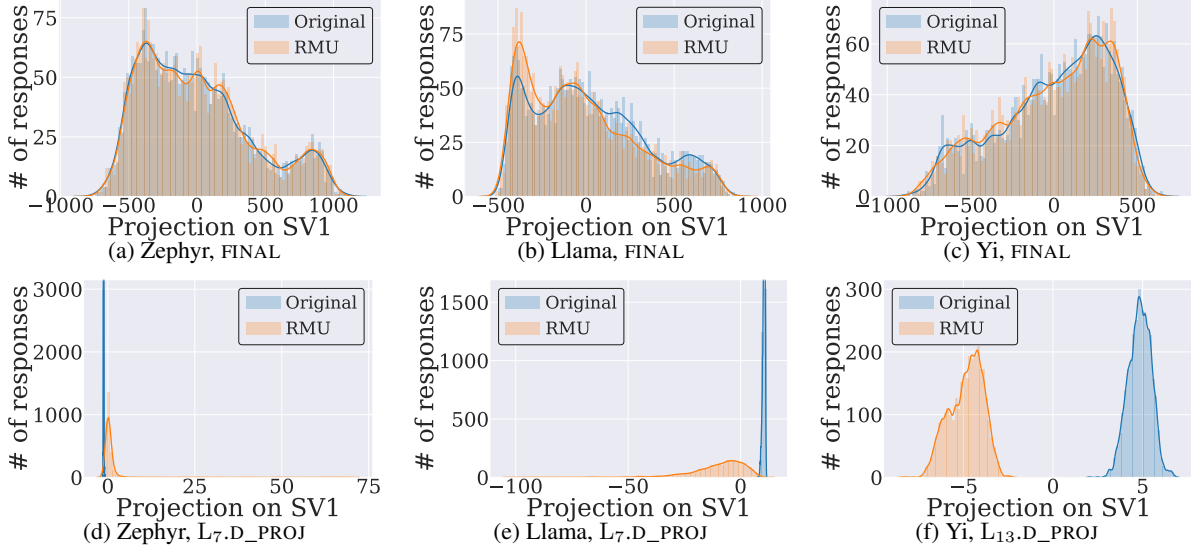


Figure 4: Projection of activations from various layers for 3000 responses to MMLU onto the top right singular vectors (denoted as SV1) for both original and unlearned models. Here, L_i .D_PROJ refers to activations extracted from the down-projection sublayer of the FFN in the i -th transformer block, while FINAL denotes the activations of the final layer after RMS-norm. (a,d) for Zephyr-7B, (b,e) for LLaMA3.1-8B, and (c,f) for Yi-34B.

activations onto the right singular vectors to visualize and analyze spectral shifts induced by unlearning. To examine how unlearning affects these internal representations, we generate 100-token responses for 3,000 randomly sampled MMLU test questions using both the original and unlearned models. Here, we focus on the most challenging unlearning trace detection scenario: identifying traces from model responses to forget-irrelevant prompts drawn from MMLU. The presence of an unlearning fingerprint is revealed through the *correct localization* of these activation shifts, which we elaborate on in the following analysis.

NPO exhibits strong spectral fingerprints. For NPO-unlearned models, we extract the final normalized activations: Specifically, the outputs from the last layer after root mean square normalization (RMSNorm). As shown in Fig. 3, there is a pronounced distributional shift between the unlearned and original models when activations are projected onto the first right singular vector (SV1). This observation aligns with the results in Tab. 3, where classifiers achieve near-perfect accuracy in distinguishing NPO-unlearned responses from those of the original model. Additional spectral fingerprint results for other models are provided in the Appendix E.

RMU exhibits subtle but clear spectral fingerprints when localized correctly. Following the same procedure, we extract the final pre-logit activations for RMU-unlearned models (denoted as FINAL). As shown in Fig. 4-(a-c), there is no apparent distributional shift in the projected activations that would allow us to distinguish the RMU-unlearned models from their original counterparts. To investigate further, we examine activations from intermediate layers, *i.e.*, the layers directly modified by RMU as described in (2).

Specifically, we extract activations from sublayers within the feed-forward network (FFN) of intermediate layers, *i.e.*, the down-projection (D_PROJ) and gate-projection (G_PROJ) sublayers. When extracting from layer i (denoted as L_i), we refer to the corresponding activations as L_i .D_PROJ and L_i .G_PROJ, respectively. As shown in Fig. 4-(d-f), all models exhibit spectral shifts in the activation distributions for responses generated by the RMU-unlearned model. For Zephyr-7B, the fingerprint appears exclusively in the projection of L_7 .D_PROJ along the first singular vector. Although present, the distributional shift is relatively subtle, validating the model’s lower classification accuracy in Tab. 2. For LLaMA3.1-8B, we again observe spectral fingerprints in L_7 .D_PROJ along the top singular direction, though the shift is more pronounced compared to Zephyr. The strongest spectral fingerprints are observed in Yi-34B, with clear shifts across multiple layers, notably L_{13} , L_{14} , and L_{15} . This observation aligns with its high classification accuracy of 95.77% in Tab. 2.

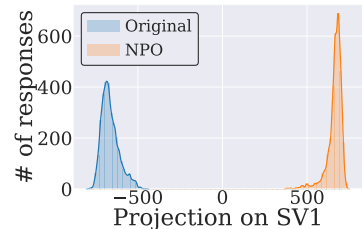


Figure 3: Projection of the final-layer normalized activations from 3,000 MMLU responses onto the first right singular vector (SV1) for the original LLaMA3.1-8B model and its NPO-unlearned counterpart.

A closer look at final activations for RMU. As shown in Fig. 4, spectral fingerprints characterized by distributional shifts were not observed in the final pre-logit activations of RMU-unlearned models. However, due to the residual stream architecture of transformers [67], earlier activations (where RMU fingerprints are found) contribute indirectly to the final output. This suggests that the unlearning signal may still be embedded in the final activations, albeit in a more complex form. To uncover this effect, we apply supervised UMAP [68], a non-linear dimensionality reduction technique. In Fig. 5, we demonstrate that UMAP yields a clearer separation between original and RMU-unlearned activations at FINAL for Zephyr-7B. Additional results for other models are presented in the Appendix F. This suggests the existence of a low-dimensional nonlinear manifold where original and unlearned final activations are well-separated, even for models like Zephyr-7B that exhibit only subtle spectral shifts in Fig. 4. This highlights the potential for learning a more effective classifier using *final pre-logit activations*, as further explored in Sec. 6.

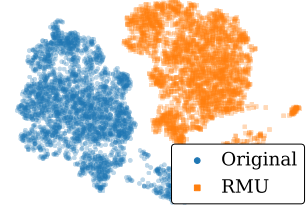


Figure 5: UMAP projections of FINAL layer activations on MMLU prompts, comparing the original and RMU-unlearned Zephyr-7B models.

6 Experiments

In this section, we present a comprehensive experimental analysis of unlearning trace detection. Our study primarily covers: (i) response-based detection under varying training data configurations and classifier architectures, (ii) an enhanced detection strategy leveraging internal model activations, and (iii) a large-scale multi-class classification across diverse model families and unlearning methods. Unless otherwise noted, all experimental setups follow those described in Sec. 4.

Supervised classification under different training regimes. Recall from Sec. 4 that the default training dataset for the supervised classifier, denoted as \mathcal{S}_{fg} , consists of a 50/50 mix of forget-related and forget-irrelevant responses. To examine how unlearning detection varies under different training data compositions, we consider two additional regimes: \mathcal{S}_f , which includes only WMDP forget-related responses (100%), and \mathcal{S}_g , which includes only MMLU forget-irrelevant responses (100%). Tab. 5 presents the performance of detecting RMU-unlearned model across the three training regimes for four LLMs. When trained solely on \mathcal{S}_f , nearly all models achieve higher accuracy on forget-related prompts (e.g., 97.20% for Zephyr-7B) compared to training on \mathcal{S}_{fg} , but their performance drops to near-random levels (around 50%) on forget-irrelevant queries. In contrast, training on \mathcal{S}_g , which lacks direct relevance to the unlearning target, fails to enable effective trace detection, even when evaluated on forget-relevant WMDP prompts. This outcome is expected, as forget-irrelevant responses used for training contain the least fingerprint information and are weakly correlated with unlearning traces. The mixed regime \mathcal{S}_{fg} , by combining both response types, consistently achieves strong performance across all evaluation scenarios. We refer the reader to the Appendix C for a parallel study on training regime effects for NPO-based unlearning trace detection.

Unlearning classification accuracy vs. choice of classifier architecture. To evaluate the impact of classifier architecture on unlearning trace detection, we compare a range of pretrained text encoders, following the protocol of [62]. Specifically, we experiment with classifiers based on BERT [66], T5 [69], GPT-2 [70], and LLM2vec [62], each paired with a lightweight two-layer MLP head. Each model is trained to distinguish between responses from the original and unlearned LLMs. As shown in Tab. 6, LLM2vec consistently achieves the highest classification accuracy across all evaluation settings, motivating its adoption as our default classifier architecture. Additional results are provided in Appendix G.

Table 5: Classification accuracy for distinguishing original vs. RMU-unlearned models under three training regimes: \mathcal{S}_{fg} , \mathcal{S}_f , and \mathcal{S}_g . Columns report test accuracy on WMDP, MMLU, and UltraChat prompts, with no overlap with the training sets.

Model	Setting	WMDP	MMLU	UltraChat
Zephyr-7B	\mathcal{S}_{fg}	90.56%	53.68%	50.14%
	\mathcal{S}_f	97.20%	51.55%	51.83%
	\mathcal{S}_g	50.00%	52.67%	50.83%
LLaMA-3.1-8B	\mathcal{S}_{fg}	93.24%	78.87%	67.60%
	\mathcal{S}_f	95.49%	51.83%	55.21%
	\mathcal{S}_g	68.45%	79.72%	69.30%
Qwen2.5-14B	\mathcal{S}_{fg}	95.07%	76.90%	65.07%
	\mathcal{S}_f	94.93%	54.08%	56.62%
	\mathcal{S}_g	73.66%	76.06%	64.37%
Yi-34B	\mathcal{S}_{fg}	94.37%	95.77%	87.46%
	\mathcal{S}_f	91.69%	61.41%	58.72%
	\mathcal{S}_g	68.73%	98.87%	84.42%

Table 6: Classification accuracy for distinguishing original vs. RMU-unlearned responses using different pretrained sequence encoders. The source LLM is Yi-34B with RMU applied on the WMDP dataset. All other settings mirror those in Tab. 2.

Classifier	WMDP	MMLU	UltraChat
LLM2vec	94.37%	95.77%	87.46%
T5	85.35%	82.96%	59.72%
GPT2	88.03%	96.06%	62.39%
BERT	88.59%	88.31%	69.15%

Improved unlearning trace detection using pre-logit activations. Recall from Sec. 5 that unlearning may leave more pronounced traces in a model’s internal representations than in its output text. To investigate this, we extract the final pre-logit activation vector for each prompt response and train a lightweight two-layer MLP classifier using these features. The training and evaluation follow the same train/test splits as used for the response-based classifiers. As shown in Fig. 6, the activation-based detector consistently and substantially outperforms the text-only approach: even in the most challenging case (Zephyr-7B on MMLU), detection accuracy for RMU unlearning improves from just over 50% to above 90%. Similar gains are observed across all models and evaluation sets. These results confirm that unlearning induces pronounced, low-dimensional shifts in the final hidden representations, which can be effectively leveraged by a simple MLP classifier. The primary limitation of this approach lies in its reliance on white-box access to extract internal activations. Additional results for other unlearning methods are provided in Appendix H.

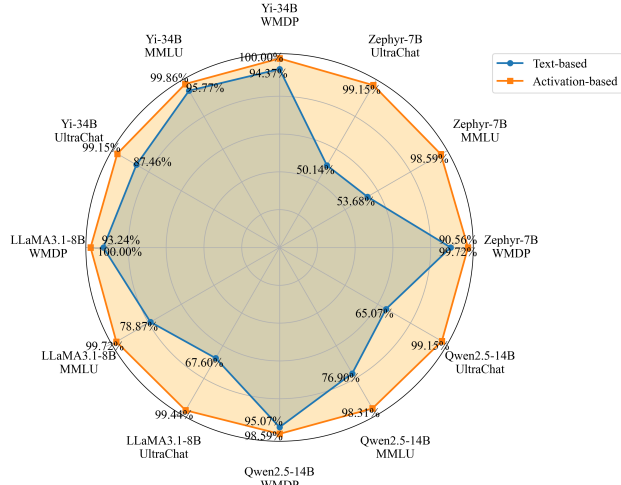


Figure 6: Radar chart comparing unlearning trace detection accuracy across four source LLMs (post-RMU unlearning) and three test sets (WMDP, MMLU, UltraChat). Classifiers are performed using two feature types: text-based responses (blue) and pre-logit activations (orange), with activation-based curves annotated at their exact values (up to 100%). The chart highlights the advantage of internal representations for robust and consistent unlearning trace detection.

Extended multi-class classification: Distinguishing unlearning variants together with source model types. We extend our analysis to a more complex 8-way classification task that jointly distinguishes among four LLM families, each in both their original and unlearned forms. This setup enables a more fine-grained examination of *model-specific unlearning traces*. Implementation and hyperparameter details are provided in Appendix I. Fig. 7 displays the resulting confusion matrices on both forget-related (WMDP) and forget-irrelevant (MMLU) test sets. On WMDP, predictions are highly concentrated along the diagonal, indicating strong agreement between the predicted and true model–unlearning pairs. This confirms that unlearning traces are clearly detectable when test prompts align with the domain of the forgotten content. In contrast, classification accuracy declines on the MMLU test set, particularly for the Zephyr-7B models, where most errors involve confusion between the original and RMU-unlearned versions. Nevertheless, larger models such as Yi-34B and Yi-34B-RMU maintain high accuracy, suggesting that unlearning traces in these models persist and remain detectable even when evaluated on general, forget-irrelevant prompts. Additional results for NPO-unlearned models under this multi-class setting are reported in Appendix I.

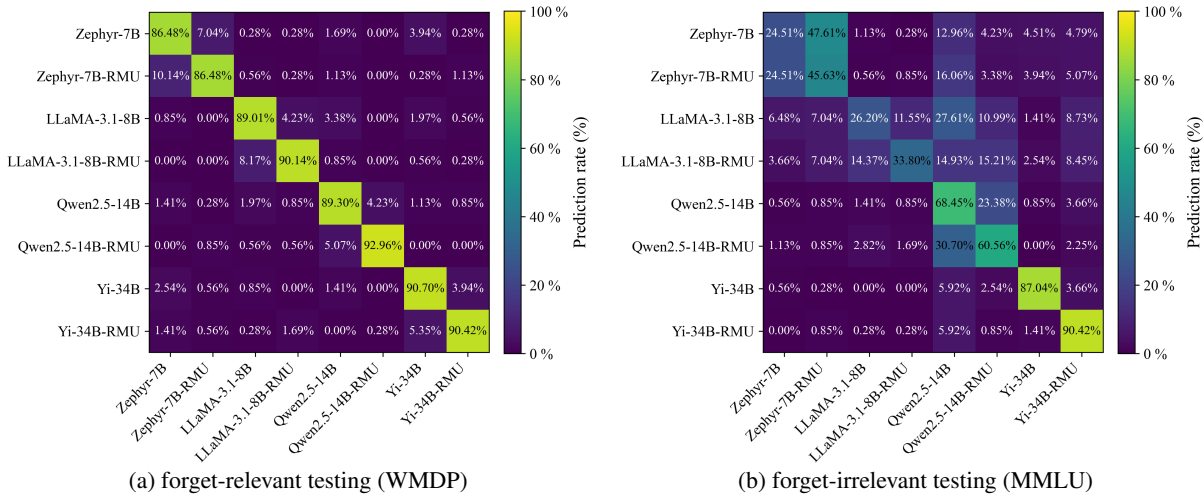


Figure 7: Confusion matrices for model–unlearning pair classification. Rows denote the true classes (*i.e.*, original or unlearned versions for each LLM type), and columns indicate the predicted classes. Diagonal entries correspond to correct predictions, while off-diagonal entries reflect misclassifications. Results are shown for (a) WMDP (forget-related) and (b) MMLU (forget-irrelevant) test sets.

7 Conclusion

We introduce and systematically study the problem of LLM unlearning trace detection, demonstrating that simple classifiers trained on model outputs have been able to distinguish unlearned models from their original counterparts. While unlearning methods such as RMU and NPO produce detectable behavioral shifts on forget-relevant prompts, RMU traces are notably harder to detect from forget-irrelevant inputs, except in larger models. Going beyond surface-level behavior, we uncover low-dimensional spectral fingerprints in hidden activations that enable near-perfect classification accuracy, even in challenging settings. These results expose a critical vulnerability: unlearning leaves persistent, learnable traces that can be exploited to reverse-engineer whether and what a model has forgotten.

8 Limitations and Broad Impacts

Limitations. While our study demonstrates the feasibility of unlearning trace detection across multiple LLM architectures and unlearning algorithms, several limitations remain that warrant future investigation. First, beyond the commonly studied RMU and NPO methods, our analysis could be extended to a broader range of unlearning techniques, which may exhibit different trace patterns and vulnerabilities. Second, our activation-based detection approach relies on white-box access to model internals, which may not be feasible in real-world deployments where access to model parameters or intermediate activations is restricted. Third, the ability to infer forgotten information from model outputs raises new concerns about the *honesty* of LLM unlearning. That is, even after unlearning, models may appear to “know” the target content without explicitly revealing it. To mitigate reverse engineering risks, future work should explore mechanisms that promote honest unlearning, for example, by encouraging models to issue explicit refusals, accompanied by grounded justifications, when queried about forgotten content. Finally, the theoretical foundations of unlearning trace detection have not been fully explored. A deeper understanding of how unlearning alters internal representations and decision boundaries is essential for formalizing detection guarantees, characterizing leakage, and guiding the design of more robust unlearning algorithms.

Broader impacts. Our ability to detect unlearning traces offers important benefits for transparency, accountability, and regulatory compliance. It enables external auditing of LLMs to verify the removal of personal data, copyrighted material, or unsafe instructions, thereby strengthening trust in unlearning as a privacy-preserving mechanism. However, this same capability introduces new risks. By analyzing model responses or internal activations, adversaries could confirm whether specific information was removed and potentially infer the nature of the forgotten content. Such reverse engineering may undermine confidentiality guarantees and expose sensitive or proprietary information. In safety-critical settings, such as biosecurity, attackers might even detect and reactivate suppressed model capabilities. To mitigate these risks, we recommend combining unlearning mechanisms with defenses such as randomized output perturbation, activation-masking layers, and formal certification protocols. These techniques can help obfuscate trace artifacts while maintaining the auditability needed for trustworthy deployment.

Acknowledgments

This work is supported by the National Science Foundation (NSF) CISE Core Program Award IIS-2207052, the NSF CAREER Award IIS-2338068, the ARO Award W911NF2310343, the Cisco Faculty Research Award, the Amazon Research Award for AI in Information Security, and an Award from the Center for AI Safety (CAIS).

References

- [1] S. Liu, Y. Yao, J. Jia, S. Casper, N. Baracaldo, P. Hase, Y. Yao, C. Y. Liu, X. Xu, H. Li *et al.*, “Rethinking machine unlearning for large language models,” *Nature Machine Intelligence*, pp. 1–14, 2025.
- [2] N. Si, H. Zhang, H. Chang, W. Zhang, D. Qu, and W. Zhang, “Knowledge unlearning for llms: Tasks, methods, and challenges,” *arXiv preprint arXiv:2311.15766*, 2023.
- [3] Y. Qu, M. Ding, N. Sun, K. Thilakarathna, T. Zhu, and D. Niyato, “The frontier of data erasure: Machine unlearning for large language models,” *arXiv preprint arXiv:2403.15779*, 2024.
- [4] A. F. Cooper, C. A. Choquette-Choo, M. Bogen, M. Jagielski, K. Filippova, K. Z. Liu, A. Chouldechova, J. Hayes, Y. Huang, N. Mireshghallah *et al.*, “Machine unlearning doesn’t do what you think: Lessons for generative ai policy, research, and practice,” *arXiv preprint arXiv:2412.06966*, 2024.
- [5] P. Regulation, “Regulation (eu) 2016/679 of the european parliament and of the council,” *Regulation (eu)*, vol. 679, p. 2016, 2016.
- [6] W. Shi, J. Lee, Y. Huang, S. Malladi, J. Zhao, A. Holtzman, D. Liu, L. Zettlemoyer, N. A. Smith, and C. Zhang, “Muse: Machine unlearning six-way evaluation for language models,” *arXiv preprint arXiv:2407.06460*, 2024.
- [7] R. Eldan and M. Russinovich, “Who’s harry potter? approximate unlearning in llms,” 2023.
- [8] Y. Yao, X. Xu, and Y. Liu, “Large language model unlearning,” in *NeurIPS*, 2024.
- [9] F. Barez, T. Fu, A. Prabhu, S. Casper, A. Sanyal, A. Bibi, A. O’Gara, R. Kirk, B. Bucknall, T. Fisteik *et al.*, “Open problems in machine unlearning for ai safety,” *arXiv preprint arXiv:2501.04952*, 2025.
- [10] Z. Zhang, J. Yang, P. Ke, S. Cui, C. Zheng, H. Wang, and M. Huang, “Safe unlearning: A surprisingly effective and generalizable solution to defend against jailbreak attacks,” *arXiv preprint arXiv:2407.02855*, 2024.
- [11] R. Shah, A. Irpan, A. M. Turner, A. Wang, A. Conmy, D. Lindner, J. Brown-Cohen, L. Ho, N. Nanda, R. A. Popa *et al.*, “An approach to technical agi safety and security,” *arXiv preprint arXiv:2504.01849*, 2025.
- [12] N. Li, A. Pan, A. Gopal, S. Yue, D. Berrios, A. Gatti, J. D. Li, A.-K. Dombrowski, S. Goel, G. Mukobi *et al.*, “The wmdp benchmark: Measuring and reducing malicious use with unlearning,” in *ICML*, 2024.
- [13] Y. Cao and J. Yang, “Towards making systems forget with machine unlearning,” in *2015 IEEE symposium on security and privacy*. IEEE, 2015, pp. 463–480.
- [14] A. Thudi, G. Deza, V. Chandrasekaran, and N. Papernot, “Unrolling sgd: Understanding factors influencing machine unlearning,” in *2022 IEEE 7th European Symposium on Security and Privacy (EuroS&P)*. IEEE, 2022, pp. 303–319.
- [15] J. Jia, J. Liu, P. Ram, Y. Yao, G. Liu, Y. Liu, P. Sharma, and S. Liu, “Model sparsity can simplify machine unlearning,” *Advances in Neural Information Processing Systems*, vol. 36, pp. 51 584–51 605, 2023.
- [16] R. Rafailov, A. Sharma, E. Mitchell, C. D. Manning, S. Ermon, and C. Finn, “Direct preference optimization: Your language model is secretly a reward model,” in *NeurIPS*, 2023.
- [17] R. Zhang, L. Lin, Y. Bai, and S. Mei, “Negative preference optimization: From catastrophic collapse to effective unlearning,” *arXiv preprint arXiv:2404.05868*, 2024.
- [18] C. Fan, J. Liu, L. Lin, J. Jia, R. Zhang, S. Mei, and S. Liu, “Simplicity prevails: Rethinking negative preference optimization for llm unlearning,” *arXiv preprint arXiv:2410.07163*, 2024.
- [19] J. Jang, D. Yoon, S. Yang, S. Cha, M. Lee, L. Logeswaran, and M. Seo, “Knowledge unlearning for mitigating privacy risks in language models,” *arXiv preprint arXiv:2210.01504*, 2022.
- [20] J. Jia, J. Liu, Y. Zhang, P. Ram, N. Baracaldo, and S. Liu, “WAGLE: Strategic weight attribution for effective and modular unlearning in large language models,” in *The Thirty-eighth Annual Conference on Neural Information Processing Systems*, 2024.
- [21] P. Hase, M. Bansal, B. Kim, and A. Ghandeharioun, “Does localization inform editing? surprising differences in causality-based localization vs. knowledge editing in language models,” *Advances in Neural Information Processing Systems*, vol. 36, pp. 17 643–17 668, 2023.
- [22] X. Wu, J. Li, M. Xu, W. Dong, S. Wu, C. Bian, and D. Xiong, “Depn: Detecting and editing privacy neurons in pretrained language models,” *arXiv preprint arXiv:2310.20138*, 2023.
- [23] J. Łucki, B. Wei, Y. Huang, P. Henderson, F. Tramèr, and J. Rando, “An adversarial perspective on machine unlearning for ai safety,” *arXiv preprint arXiv:2409.18025*, 2024.
- [24] A. Lynch, P. Guo, A. Ewart, S. Casper, and D. Hadfield-Menell, “Eight methods to evaluate robust unlearning in llms,” *arXiv preprint arXiv:2402.16835*, 2024.

- [25] S. Hu, Y. Fu, S. Wu, and V. Smith, "Jogging the memory of unlearned models through targeted relearning attacks," in *ICML 2024 Workshop on Foundation Models in the Wild*, 2024.
- [26] A. Deeb and F. Roger, "Do unlearning methods remove information from language model weights?" *arXiv preprint arXiv:2410.08827*, 2024.
- [27] Defense Advanced Research Projects Agency (DARPA), "Reverse engineering of deceptions (red)," 2021, accessed: 2025-05-14. [Online]. Available: <https://www.darpa.mil/research/programs/reverse-engineering-of-deceptions>
- [28] Y. Yao, Y. Gong, Y. Li, Y. Zhang, X. Lin, and S. Liu, "Reverse engineering of imperceptible adversarial image perturbations," in *International Conference on Learning Representations*, 2022.
- [29] Y. Yao, X. Guo, V. Asnani, Y. Gong, J. Liu, X. Lin, X. Liu, S. Liu *et al.*, "Reverse engineering of deceptions on machine-and human-centric attacks," *Foundations and Trends® in Privacy and Security*, vol. 6, no. 2, pp. 53–152, 2024.
- [30] C. J. Hoofnagle, B. van der Sloot, and F. Z. Borgesius, "The european union general data protection regulation: what it is and what it means," *Information & Communications Technology Law*, vol. 28, no. 1, pp. 65–98, 2019.
- [31] L. Bourtole, V. Chandrasekaran, C. A. Choquette-Choo, H. Jia, A. Travers, B. Zhang, D. Lie, and N. Papernot, "Machine unlearning," in *2021 IEEE Symposium on Security and Privacy (SP)*. IEEE, 2021, pp. 141–159.
- [32] T. T. Nguyen, T. T. Huynh, P. L. Nguyen, A. W.-C. Liew, H. Yin, and Q. V. H. Nguyen, "A survey of machine unlearning," *arXiv preprint arXiv:2209.02299*, 2022.
- [33] Y. Zhang, J. Jia, X. Chen, A. Chen, Y. Zhang, J. Liu, K. Ding, and S. Liu, "To generate or not? safety-driven unlearned diffusion models are still easy to generate unsafe images... for now," in *European Conference on Computer Vision*. Springer, 2024, pp. 385–403.
- [34] Y. Zhang, X. Chen, J. Jia, Y. Zhang, C. Fan, J. Liu, M. Hong, K. Ding, and S. Liu, "Defensive unlearning with adversarial training for robust concept erasure in diffusion models," *Advances in Neural Information Processing Systems*, vol. 37, pp. 36 748–36 776, 2024.
- [35] Y. Zhang, Y. Zhang, Y. Yao, J. Jia, J. Liu, X. Liu, and S. Liu, "Unlearncanvas: A stylized image dataset to benchmark machine unlearning for diffusion models," *arXiv preprint arXiv:2402.11846*, 2024.
- [36] J. Jia, Y. Zhang, Y. Zhang, J. Liu, B. Runwal, J. Diffenderfer, B. Kaikhura, and S. Liu, "Soul: Unlocking the power of second-order optimization for llm unlearning," *arXiv preprint arXiv:2404.18239*, 2024.
- [37] Y. Chen, Y. Yao, Y. Zhang, B. Shen, G. Liu, and S. Liu, "Safety mirage: How spurious correlations undermine vlm safety fine-tuning," *arXiv preprint arXiv:2503.11832*, 2025.
- [38] G. Ilharco, M. T. Ribeiro, M. Wortsman, S. Gururangan, L. Schmidt, H. Hajishirzi, and A. Farhadi, "Editing models with task arithmetic," *arXiv preprint arXiv:2212.04089*, 2022.
- [39] Y. Yao, X. Xu, and Y. Liu, "Large language model unlearning," *arXiv preprint arXiv:2310.10683*, 2023.
- [40] J. Chen and D. Yang, "Unlearn what you want to forget: Efficient unlearning for llms," *arXiv preprint arXiv:2310.20150*, 2023.
- [41] P. Maini, Z. Feng, A. Schwarzschild, Z. C. Lipton, and J. Z. Kolter, "Tofu: A task of fictitious unlearning for llms," 2024.
- [42] K. Meng, D. Bau, A. Andonian, and Y. Belinkov, "Locating and editing factual associations in gpt," *Advances in Neural Information Processing Systems*, vol. 35, pp. 17 359–17 372, 2022.
- [43] C. Yu, S. Jeoung, A. Kasi, P. Yu, and H. Ji, "Unlearning bias in language models by partitioning gradients," in *Findings of the Association for Computational Linguistics: ACL 2023*, 2023, pp. 6032–6048.
- [44] P. Thaker, Y. Maurya, and V. Smith, "Guardrail baselines for unlearning in llms," *arXiv preprint arXiv:2403.03329*, 2024.
- [45] M. Pawelczyk, S. Neel, and H. Lakkaraju, "In-context unlearning: Language models as few shot unlearners," *arXiv preprint arXiv:2310.07579*, 2023.
- [46] M. Sun, Y. Yin, Z. Xu, J. Z. Kolter, and Z. Liu, "Idiosyncrasies in large language models," *arXiv preprint arXiv:2502.12150*, 2025.
- [47] S. Zhu, A. Ahmed, R. Kudithipudi, and P. Liang, "Independence tests for language models," *arXiv preprint arXiv:2502.12292*, 2025.
- [48] M. Lamparth and A. Reuel, "Analyzing and editing inner mechanisms of backdoored language models," in *Proceedings of the 2024 ACM Conference on Fairness, Accountability, and Transparency*, 2024, pp. 2362–2373.

- [49] N. M. Min, L. H. Pham, Y. Li, and J. Sun, "Crow: Eliminating backdoors from large language models via internal consistency regularization," *arXiv preprint arXiv:2411.12768*, 2024.
- [50] B. Tran, J. Li, and A. Madry, "Spectral signatures in backdoor attacks," *Advances in neural information processing systems*, vol. 31, 2018.
- [51] J. Hayase, W. Kong, R. Somani, and S. Oh, "Spectre: defending against backdoor attacks using robust statistics," in *Proceedings of the 38th International Conference on Machine Learning*, ser. Proceedings of Machine Learning Research, M. Meila and T. Zhang, Eds., vol. 139. PMLR, 18–24 Jul 2021, pp. 4129–4139. [Online]. Available: <https://proceedings.mlr.press/v139/hayase21a.html>
- [52] D. Tang, X. Wang, H. Tang, and K. Zhang, "Demon in the variant: Statistical analysis of {DNNs} for robust backdoor contamination detection," in *30th USENIX Security Symposium (USENIX Security 21)*, 2021, pp. 1541–1558.
- [53] W. Chen, B. Wu, and H. Wang, "Effective backdoor defense by exploiting sensitivity of poisoned samples," in *Advances in Neural Information Processing Systems*, A. H. Oh, A. Agarwal, D. Belgrave, and K. Cho, Eds., 2022. [Online]. Available: <https://openreview.net/forum?id=AsH-Tx2U0Ug>
- [54] Y. Gong, Y. Yao, Y. Li, Y. Zhang, X. Liu, X. Lin, and S. Liu, "Reverse engineering of imperceptible adversarial image perturbations," *arXiv preprint arXiv:2203.14145*, 2022.
- [55] X. Lu, S. Welleck, J. Hessel, L. Jiang, L. Qin, P. West, P. Ammanabrolu, and Y. Choi, "Quark: Controllable text generation with reinforced unlearning," in *NeurIPS*, 2022.
- [56] R. Zhang, L. Lin, Y. Bai, and S. Mei, "Negative preference optimization: From catastrophic collapse to effective unlearning," in *CoLM*, 2024.
- [57] D. Hendrycks, C. Burns, S. Basart, A. Zou, M. Mazeika, D. Song, and J. Steinhardt, "Measuring massive multitask language understanding," *arXiv preprint arXiv:2009.03300*, 2020.
- [58] L. Zheng, W.-L. Chiang, Y. Sheng, S. Zhuang, Z. Wu, Y. Zhuang, Z. Lin, Z. Li, D. Li, E. Xing *et al.*, "Judging llm-as-a-judge with mt-bench and chatbot arena," in *NeurIPS*, 2023.
- [59] F. Qi, Y. Chen, M. Li, Y. Yao, Z. Liu, and M. Sun, "Onion: A simple and effective defense against textual backdoor attacks," in *EMNLP*, 2021, pp. 9558–9566.
- [60] D. Hendrycks, C. Burns, S. Basart, A. Zou, M. Mazeika, D. Song, and J. Steinhardt, "Measuring massive multitask language understanding," in *ICLR*, 2020.
- [61] N. Ding, Y. Chen, B. Xu, Y. Qin, S. Hu, Z. Liu, M. Sun, and B. Zhou, "Enhancing chat language models by scaling high-quality instructional conversations," in *EMNLP*, 2023, pp. 3029–3051.
- [62] P. BehnamGhader, V. Adlakha, M. Mosbach, D. Bahdanau, N. Chapados, and S. Reddy, "Llm2vec: Large language models are secretly powerful text encoders," in *CoLM*, 2024.
- [63] C.-Y. Lin, "Rouge: A package for automatic evaluation of summaries," in *Text summarization branches out*, 2004, pp. 74–81.
- [64] C.-Y. Lin and F. J. Och, "Automatic evaluation of machine translation quality using longest common subsequence and skip-bigram statistics," in *Proceedings of the 42nd annual meeting of the association for computational linguistics (ACL-04)*, 2004, pp. 605–612.
- [65] T. Zhang, V. Kishore, F. Wu, K. Q. Weinberger, and Y. Artzi, "Bertscore: Evaluating text generation with bert," *arXiv preprint arXiv:1904.09675*, 2019.
- [66] J. Devlin, M.-W. Chang, K. Lee, and K. Toutanova, "Bert: Pre-training of deep bidirectional transformers for language understanding," in *NAACL*, 2019, pp. 4171–4186.
- [67] N. Elhage, N. Nanda, C. Olsson, T. Henighan, N. Joseph, B. Mann, A. Askell, Y. Bai, A. Chen, T. Conerly *et al.*, "A mathematical framework for transformer circuits," *Transformer Circuits Thread*, vol. 1, no. 1, p. 12, 2021.
- [68] L. McInnes, J. Healy, and J. Melville, "Umap: Uniform manifold approximation and projection for dimension reduction," *arXiv preprint arXiv:1802.03426*, 2018.
- [69] C. Raffel, N. Shazeer, A. Roberts, K. Lee, S. Narang, M. Matena, Y. Zhou, W. Li, and P. J. Liu, "Exploring the limits of transfer learning with a unified text-to-text transformer," *JMLR*, 2020.
- [70] A. Radford, J. Wu, R. Child, D. Luan, D. Amodei, I. Sutskever *et al.*, "Language models are unsupervised multitask learners," *OpenAI blog*, 2019.

Appendix

A Unlearning Configuration and Data Preparation

Unlearning setups. We apply both RMU and NPO unlearning algorithms to four LLMs (Zephyr-7B, Llama-3.1-8B, Qwen2.5-7B, and Yi-34B) using the WMDP benchmark. To evaluate forget utility, we evaluate each unlearned model on both the WMDP-bio and WMDP-cyber subsets, while in order to assess general utility, we measure performance on MMLU. The results are summarized in **Tab. A1**.

For RMU unlearning of the Zephyr-7B model, we set the control scaling factor c in Eq. (2) to 6.5, $\gamma = 1200$. Then we perform unlearning by optimizing layer 5,6,7 while calculating the unlearning loss in Eq. (1) using the seventh intermediate layer of M_θ . For Llama-3.1-8B, scaling factor is set to 45, $\gamma = 1300$ and the other settings are consistent with the Zephyr-7B model. For the Qwen2.5-14B model, we set $c = 460$, $\gamma = 350$. The unlearning loss in Eq. (1) is computed using the activations immediately following the tenth intermediate layer and we perform parameter updates on layers 8,9,10. Finally, for Yi-34B-Chat, $c = 300$, $\gamma = 350$ and unlearning is performed exclusively on the layers 13, 14 and 15 using activations from the fifteenth intermediate layer.

For NPO, we perform unlearning for 140 steps with a batch size of 4. For different models, we use different learning rates and different utility regularization γ in Eq. (3) and present these setups in **Tab. A2**.

Classification data construction. To generate both forget and forget-irrelevant responses from each model, we first extracted the questions from the WMDP, MMLU, and UltraChat datasets. For UltraChat forget-irrelevant examples, we provided only the question itself. Similarly for the WMDP “forget” questions, we provide only the question and task the LLM to generate the corresponding answer. Only for MMLU, since much of the semantic content resides in the answer choices, we retrieved the question together with its choices and used the following prompt:

```
messages = [
  {
    "role": "user",
    "content": (
      f"{question}\n"
      f"{choices}\n\n"
      "Please provide your analysis, then give the final answer.\n\n"
      "Analysis:"
    )
  }
]
```

B Classifier Training Protocol

Data splits. We investigate classifier performance under three training regimes:

- S_{fg} : An equal mixture of WMDP (forget) responses and MMLU (forget-irrelevant) responses. We randomly sample 2,900 questions from each benchmark, collect the corresponding model responses, and train on the combined 5,800 sample sets.
- S_f : only WMDP (forget) responses which come from 2,900 question samples.
- S_g : only MMLU (forget-irrelevant) responses which come from 5,800 question samples.

To assess generalization, we hold out 355 unseen questions and their responses from each benchmark, which is disjoint from all training set, and evaluate the classifier on the three test subsets, which includes MMLU, WMDP and UltraChat.

Table A1: Unlearning effectiveness is measured on WMDP and general utility on MMLU for each LLM after applying RMU and NPO unlearning on WMDP. Both evaluations report the accuracy on four-choice question answering.

Model	WMDP-bio	WMDP-cyber	MMLU
Zephyr-7B	64.65%	44.44%	58.49%
+RMU	30.64%	27.78%	57.45%
+NPO	24.82%	37.09%	48.01%
Llama-3.1-8B	69.84%	43.94%	63.36%
+RMU	38.75%	25.06%	59.64%
+NPO	26.86%	37.24%	54.59%
Qwen2.5-14B	80.54%	52.99%	77.56%
+RMU	29.69%	26.72%	76.16%
+NPO	39.43%	45.94%	72.09%
Yi-34B-Chat	74.00%	49.27%	72.35%
+RMU	30.79%	28.59%	70.63%
+NPO	32.91%	30.39%	41.54%

Table A2: Unlearning Setup for NPO. γ refers to the utility regularization.

Model	Learning Rate	γ
Zephyr-7B	7e-06	1.0
Llama-3.1-8B	2e-05	2.0
Qwen2.5-14B	7e-05	1.0
Yi-34B	6e-05	1.0

Classifier training details. In our classifier architecture, we adopt LLM2vec as our base encoder, a lightweight sentence-level model tailored for open-ended LLM outputs, and append a two-layer MLP head to produce logits over the binary label space (original vs. unlearned). All experiments were conducted on an NVIDIA A6000 GPU. We fine-tune the entire network end-to-end under a standard supervised learning protocol, training for three epochs with AdamW (weight decay 0.001) and a cosine decay schedule (initial learning rate 8×10^{-5} , warmup ratio 0.1). We use a batch size of 8, mixed-precision BF16, gradient clipping at 0.3, and enable gradient checkpointing to reduce memory usage. All data splits and random seeds (42) for sampling, initialization, and shuffling are fixed for reproducibility.

C Detection of NPO Unlearning under Different Training Regimes

Table A3: Classification accuracy for distinguishing original vs. NPO-unlearned responses under three training regimes: \mathcal{S}_{fg} , \mathcal{S}_f , and \mathcal{S}_g . All experiments use four LLMs with NPO unlearning applied on the WMDP dataset. The settings are consistent with Tab. 5.

Model	Setting	WMDP	MMLU	UltraChat
Zephyr-7B	\mathcal{S}_{fg}	99.72%	99.86%	99.16%
	\mathcal{S}_f	100%	99.58%	98.73%
	\mathcal{S}_g	99.72%	100%	99.15%
LLaMA-3.1-8B	\mathcal{S}_{fg}	100%	99.72%	99.72%
	\mathcal{S}_f	99.72%	98.03%	97.46%
	\mathcal{S}_g	100%	85.93%	99.72%
Qwen2.5-14B	\mathcal{S}_{fg}	99.72%	99.72%	99.44%
	\mathcal{S}_f	99.72%	99.44%	99.15%
	\mathcal{S}_g	99.86%	99.72%	99.86%
Yi-34B	\mathcal{S}_{fg}	99.86%	98.87%	99.15%
	\mathcal{S}_f	99.86%	99.86%	98.45%
	\mathcal{S}_g	99.72%	100%	99.58%

In contrast to RMU (Tab. 5), NPO traces are so pronounced that classification accuracy remains near-perfect (>97 %) under all three training regimes. As shown in **Tab. A3**, even when the classifier is trained exclusively on forget-irrelevant MMLU data (\mathcal{S}_g), it still achieves over 99% accuracy on WMDP “forget” prompts, and above 98% on UltraChat for all models. Training on forget-only data (\mathcal{S}_f) likewise yields over 97% detection on “forget irrelevant” prompts. The mixed regime (\mathcal{S}_{fg}) offers no substantial benefit over the single-domain regimes, underscoring that NPO’s aggressive output artifacts are easily learned regardless of training composition. By comparison, RMU required mixed-domain exposure to reach robust performance (Sec. 6), highlighting the fundamentally stronger and domain-agnostic nature of NPO unlearning traces.

D Illustrative Response of Original vs. Unlearned Models

Tab. A4 presents representative outputs from the original Yi-34B model alongside its RMU- and NPO-unlearned variants under two types of prompts: (1) a “forget” prompt drawn from the WMDP evaluation set, which tests the model’s ability to omit specific target knowledge, and (2) a “forget-irrelevant” multiple-choice question adapted from MMLU, which assesses general question-answering behavior. Notice that both unlearning methods induce highly incoherent or truncated text when responding to the forget prompt, but the NPO-unlearned model exhibits even more extreme token-level garbling and repeated punctuation than RMU. In contrast, on the forget-irrelevant prompt, RMU produces fully fluent answers, whereas NPO occasionally introduces minor formatting artifacts.

Tab. A5 reports analogous comparisons for Zephyr-7B and its RMU- and NPO-unlearned variants. Both unlearning methods severely disrupt the forget-prompt response—RMU yields semi-coherent but heavily garbled fragments, while NPO collapses into extended runs of punctuation and nonsensical tokens. Crucially, across both Yi-34B and Zephyr-7B, NPO always induces more aggressive degradation than RMU: even though both unlearned models produce correct answer selections on the MMLU-style “forget-irrelevant” prompt, NPO’s generated text exhibits a higher incidence of raw, undecoded token sequences and formatting artifacts. This pattern holds despite preserved selection accuracy, demonstrating that NPO shifts the answer generation behavior more radically than RMU while leaving the surface choice unaffected.

E Detailed Spectral Fingerprints

Spectral fingerprints for NPO-unlearned models. In **Fig. A1**, we present the spectral fingerprints of models unlearned using NPO, using activations of the last layer after normalization. Consistent with our observations in Sec. 5,

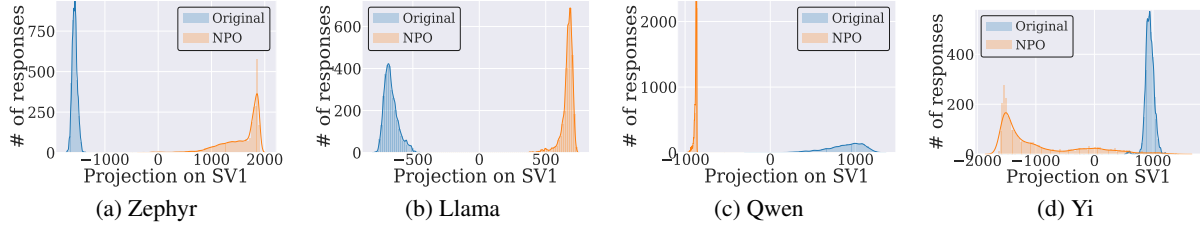


Figure A1: Projection of the final-layer normalized activations from 3,000 MMLU responses onto the first right singular vector (SV1) for the original and its NPO-unlearned counterpart. (a) is projection for Zephyr-7B, (b) for Llama3.1-8B, (c) for Qwen2.5-14B, (d) for Yi-34B.

$L_{15}.D_PROJ$ projected onto the top right singular vector, where the spectral shift is especially pronounced in the first two.

F A Closer Look at Final Activations

Similar to Sec. 5, we present the supervised UMAP projections of the final activations from different models in Fig. A4. Consistent with Sec. 5, UMAP always yields clear separation between the original and RMU-unlearned activations.

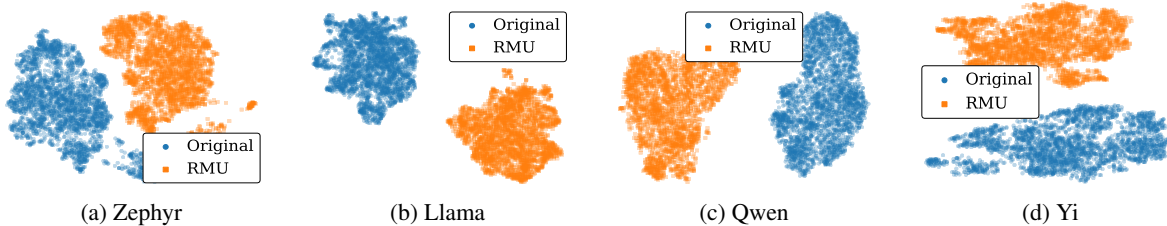


Figure A4: Supervised UMAP Projections of the final-layer normalized activations from 3,000 MMLU responses for the original and its RMU-unlearned counterpart using (a) Zephyr-7B, (b) Llama3.1-8B, (c) Qwen2.5-14B, (d) Yi-34B-Chat.

G Effect of Pretrained Encoder on Classifier Performance

To further probe how unlearning strength affects trace detectability across encoder architectures, we repeat our classification evaluation under the same mixed regime (S_{fg}) for both RMU- and NPO-unlearned Yi-34B outputs. Tab. 6 and Tab. A6 report accuracy when distinguishing original from unlearned responses using four different pretrained encoders. For RMU unlearning (Tab. 6), all encoders perform well on the WMDP “forget” data and MMLU “forget-irrelevant” data, but LLM2vec achieves the highest overall robustness, especially on UltraChat, where it attains 87.46% accuracy versus below 70% for the others. This validates our choice of LLM2vec as the default detector when unlearning traces are relatively subtle.

Table A6: Classification accuracy for distinguishing original vs. NPO-unlearned responses using different pretrained sequence encoders. The other settings are consistent with Tab. 6.

Classifier	WMDP	MMLU	UltraChat
LLM2vec	99.86%	98.87%	99.15%
T5	99.29%	99.30%	86.20%
GPT2	99.72%	99.86%	96.90%
BERT	99.44%	99.58%	94.65%

In stark contrast, Tab. A6 describes NPO unlearning yields near-perfect detection across both prompt types and all domains. Even the least robust encoder (T5) attains over 86% on UltraChat, while LLM2vec, GPT-2, and BERT all exceed 94% everywhere, with LLM2vec surpassing 99% on every test. This demonstrates that NPO’s more aggressive unlearning introduces globally visible artifacts, like raw token fragments and formatting anomalies, that make trace detection trivial, even on “forget-irrelevant” prompts where RMU traces often remain hidden.

H Improved Unlearning Detection using Activations

Tab. A7 reports unlearning classification accuracy when using RMS-normalized final pre-logit activations as input to a two-layer MLP, compared against our text-based baseline (Tab. 2). Across all four source LLMs (Yi-34B, Zephyr-7B, Llama-3.1-8B, and Qwen2.5-14B) and three test sets (WMDP, MMLU, UltraChat), activation-based features yield a

substantial gain as elaborated on below. 1. Worst-case improvement: For Zephyr-7B on MMLU, detection jumps from just 53% (text) to 98% (activations), over 40% increase. 2. Consistent gains on “forget-irrelevant”: On UltraChat, where text signals are most subtle, accuracy rises across all models. 3. Overall robustness: The mean accuracy across all twelve evaluation points increases, demonstrating that unlearning traces are more linearly separable in activation space. These results confirm that the final pre-logit activations encode stronger, model-internal signatures of unlearning than the raw text outputs alone. The primary drawback is the requirement for white-box access to extract these activations, which may not be feasible in every deployment scenario.

Tab. A8 and **Fig. A5** shows the results for NPO unlearning detection using the activations. Text-based classifiers (marked using blue in **Fig. A5**) already achieve high accuracy, often above 99% in distinguishing original from NPO-unlearned responses, reflecting the presence of unlearning artifacts in the text. Consequently, activation-based features (orange) have relatively limited headroom for improvement, pushing models to a ceiling of 99–100% across all tasks. This narrow margin confirms that NPO traces are so pronounced in the text itself that final-layer embeddings offer only incremental gains.

While activation-based detection consistently achieves near-perfect accuracy for both RMU and NPO unlearning methods, it requires white-box access to the model’s internal states, specifically, the ability to extract final-layer activation features. This introduces practical constraints in real-world applications, where such internal access may be unavailable or restricted. In the case of RMU, text-based classifiers often exhibit limitations, particularly on “forget-irrelevant” prompts, inputs that do not explicitly reference the forgotten information but can still reveal unlearning traces through nuanced generation patterns. For these harder cases, activation features serve as a robust fallback, enabling over 30% improvement in worst-case detection performance. By contrast, NPO exhibits much stronger performance under text-based detection alone, achieving approximately 99% accuracy across all prompt types. This leaves minimal headroom for further improvement using activation-based signals, which tend to saturate close to the same level. In summary, activation-based classifiers are highly effective when white-box access is available, especially for RMU. But in black-box settings, text-based methods remain the most practical and scalable solution.

I Multi-Class Classification Results

Compared to the heatmaps shown in **Fig. 7** of the main text, the exact percentages in **Tab. A9** and **Tab. A10** make it clear that on WMDP prompts the classifier’s accuracy is tightly clustered along the diagonal (all models between 86–93%), with only small off-diagonal swaps (7%–10% for Zephyr, <6% for others). On MMLU, the Zephyr pair’s diagonal entries (24.5% vs. 45.6%) correspond exactly to the heavy confusion blocks seen in **Fig. 7(b)**, while the Yi-34B and Qwen2.5-7B series retain visibly brighter diagonal cells, matching their stronger separation in the heatmap. Thus, the tables quantify the same model-and-unlearn differentials that the main-text figures visually highlight.

The NPO confusion matrices in **Tab. A11** and **Tab. A12** reveal a dramatic improvement over RMU (**Tab. A9**, **Tab. A10**). On WMDP “forget” prompts, correct-classification rates for original models rise from 86.48% (Zephyr-7B under RMU)

Table A7: Classification accuracy using RMS-normalized final-layer activations to distinguish original vs. RMU-unlearned responses (unlearning applied on WMDP). All other settings mirror those in **Tab. 2**.

Model	WMDP	MMLU	UltraChat
Zephyr-7B	99.72%	98.59%	99.15%
LLaMA-3.1-8B	100%	99.72%	99.44%
Qwen2.5-14B	98.59%	98.31%	99.15%
Yi-34B	100%	99.86%	99.86%

Table A8: Classification accuracy using RMS-normalized final-layer activations to distinguish original vs. NPO-unlearned responses (unlearning applied on WMDP). All other settings mirror those in **Tab. 3**.

Model	WMDP	MMLU	UltraChat
Zephyr-7B	100%	99.86%	99.86%
LLaMA-3.1-8B	100%	100%	99.44%
Qwen2.5-14B	99.86%	99.44%	99.44%
Yi-34B	99.72%	99.86%	99.86%

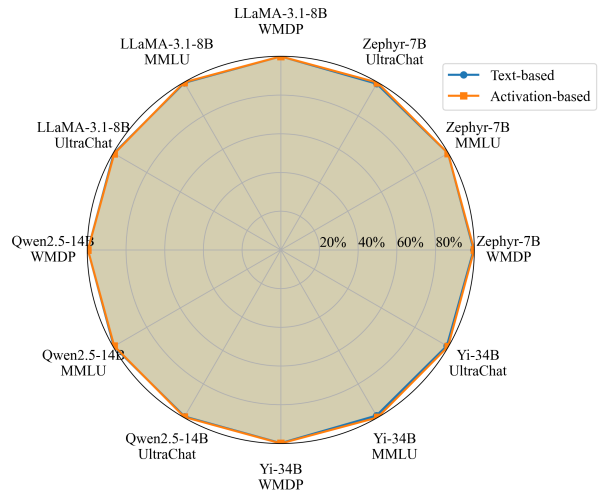


Figure A5: Radar chart comparing NPO-unlearning detection accuracy using text-based responses (blue) versus pre-logit activation features (orange) across four LLMs on three test sets.

Table A9: Confusion matrix (row-normalized percentages) for RMU unlearning detection given WMDP prompts. Rows indicate true classes (original/unlearned model variants), and columns show predicted classes. Diagonal entries represent correct predictions; off-diagonals indicate misclassification rates.

True \ Pred	Zephyr-7B	Zephyr-7B-RMU	Yi-34B-Chat	Yi-34B-Chat-RMU	LLaMA-3.1-8B	LLaMA-3.1-8B-RMU	Qwen2.5-14B	Qwen2.5-14B-RMU
Zephyr-7B	86.48%	7.04%	3.94%	0.28%	0.28%	0.28%	1.69%	0.00%
Zephyr-7B-RMU	10.14%	86.48%	0.28%	1.13%	0.56%	0.28%	1.13%	0.00%
Yi-34B-Chat	2.54%	0.56%	90.70%	3.94%	0.85%	0.00%	1.41%	0.00%
Yi-34B-Chat-RMU	1.41%	0.56%	5.35%	90.42%	0.28%	1.69%	0.00%	0.28%
LLaMA-3.1-8B	0.85%	0.00%	1.97%	0.56%	89.01%	4.23%	3.38%	0.00%
LLaMA-3.1-8B-RMU	0.00%	0.00%	0.56%	0.28%	8.17%	90.14%	0.85%	0.00%
Qwen2.5-14B	1.41%	0.28%	1.13%	0.85%	1.97%	0.85%	89.30%	4.23%
Qwen2.5-14B-RMU	0.00%	0.85%	0.00%	0.00%	0.56%	0.56%	5.07%	92.96%

Table A10: Confusion matrix (row-normalized percentages) for RMU unlearning detection given MMLU prompts. The other settings are consistent with Tab. A9.

True \ Pred	Zephyr-7B	Zephyr-7B-RMU	Yi-34B-Chat	Yi-34B-Chat-RMU	LLaMA-3.1-8B	LLaMA-3.1-8B-RMU	Qwen2.5-7B	Qwen2.5-7B-RMU
Zephyr-7B	24.51%	47.61%	4.51%	4.79%	1.13%	0.28%	12.96%	4.23%
Zephyr-7B-RMU	24.51%	45.63%	3.94%	5.07%	0.56%	0.85%	16.06%	3.38%
Yi-34B-Chat	0.56%	0.28%	87.04%	3.66%	0.00%	0.00%	5.92%	2.54%
Yi-34B-Chat-RMU	0.00%	0.85%	1.41%	90.42%	0.28%	0.28%	5.92%	0.85%
LLaMA-3.1-8B	6.48%	7.04%	1.41%	8.73%	26.20%	11.55%	27.61%	10.99%
LLaMA-3.1-8B-RMU	3.66%	7.04%	2.54%	8.45%	14.37%	33.80%	14.93%	15.21%
Qwen2.5-7B	0.56%	0.85%	0.85%	3.66%	1.41%	0.85%	68.45%	23.38%
Qwen2.5-7B-RMU	1.13%	0.85%	0.00%	2.25%	2.82%	1.69%	30.70%	60.56%

Table A11: Row-normalized confusion matrix for 8-way classification of original vs. NPO-unlearned models on WMDP “forget” prompts. Each row sums to 100 %, bold diagonal entries are correct classifications.

True \ Pred	Zephyr-7B	Zephyr-7B-NPO	Yi-34B	Yi-34B-NPO	LLaMA-3.1-8B	LLaMA-3.1-8B-NPO	Qwen2.5-14B	Qwen2.5-14B-NPO
Zephyr-7B	94.08%	0.00%	3.10%	0.00%	1.13%	0.00%	1.69%	0.00%
Zephyr-7B-NPO	0.00%	100.00%	0.00%	0.00%	0.00%	0.00%	0.00%	0.00%
Yi-34B	4.79%	0.00%	90.42%	0.00%	1.13%	0.00%	3.66%	0.00%
Yi-34B-NPO	0.00%	0.00%	0.00%	99.72%	0.28%	0.00%	0.00%	0.00%
LLaMA-3.1-8B	0.28%	0.00%	2.25%	0.00%	92.68%	0.00%	4.79%	0.00%
LLaMA-3.1-8B-NPO	0.00%	0.00%	0.00%	0.00%	0.00%	100.00%	0.00%	0.00%
Qwen2.5-14B	1.13%	0.00%	1.13%	0.00%	2.54%	0.00%	95.21%	0.00%
Qwen2.5-14B-NPO	0.00%	0.00%	0.00%	0.00%	0.00%	0.00%	0.00%	100.00%

Table A12: Row-normalized confusion matrix for 8-way classification of original vs. NPO-unlearned models, evaluated on mixed MMLU prompts. Each row sums to 100%; bold diagonal entries are correct classifications.

True \ Pred	Zephyr-7B	Zephyr-7B-NPO	Yi-34B	Yi-34B-NPO	LLaMA-3.1-8B	LLaMA-3.1-8B-NPO	Qwen2.5-14B	Qwen2.5-14B-NPO
Zephyr-7B	96.34%	0.00%	1.13%	0.00%	1.41%	0.00%	1.13%	0.00%
Zephyr-7B-NPO	0.00%	99.72%	0.00%	0.00%	0.28%	0.00%	0.00%	0.00%
Yi-34B	0.85%	0.00%	97.18%	0.00%	0.28%	0.00%	1.69%	0.00%
Yi-34B-NPO	0.00%	0.00%	0.00%	100.00%	0.00%	0.00%	0.00%	0.00%
LLaMA-3.1-8B	2.25%	0.85%	0.00%	0.00%	95.77%	0.00%	1.13%	0.00%
LLaMA-3.1-8B-NPO	0.00%	0.00%	0.00%	0.00%	0.00%	100.00%	0.00%	0.00%
Qwen2.5-14B	1.13%	0.00%	0.28%	0.00%	4.79%	0.00%	93.80%	0.00%
Qwen2.5-14B-NPO	0.00%	0.00%	0.00%	0.00%	0.00%	0.00%	0.56%	99.44%

up to 94.08% under NPO, with every NPO variant achieving 100.00% accuracy. Under RMU, smaller models like Zephyr-7B and LLaMA-3.1-8B suffered off-diagonal swaps of up to 10%, whereas NPO reduces all confusion to under 4%. On MMLU “forget-irrelevant” prompts, NPO elevates Zephyr-7B accuracy from 24.51% (RMU) to 96.34%, and LLaMA-3.1-8B from 26.20% to 95.77%. Even larger models see substantial gains: Yi-34B-Chat climbs from 87.04% to 97.18%, and Qwen2.5-14B from 68.45% to 93.80%. These results confirm that NPO unlearning imprints strong, domain-agnostic artifacts that make multi-class identification virtually perfect, in stark contrast to RMU’s more subtle and domain-dependent traces. Fig. A6 makes the NPO results visually striking. In panel (a), nearly every cell off the main diagonal is almost entirely dark, indicating that the classifier almost never confuses one class for another on WMDP “forget” prompts. The diagonal band itself is uniformly bright, reflecting the over 94% correct classification rates seen in Tab. A11. Panel (b) shows a similarly unbroken diagonal on MMLU “forget-irrelevant” prompts, even Zephyr-7B, which under RMU had its signal buried in off-diagonals, now appears as a clean, high contrast stripe. The absence of any noticeable off-diagonal “leakage” in both panels underscores how aggressively NPO imprints a unique, domain-agnostic behavioral signature into every model variant, rendering multi-class identification effectively.

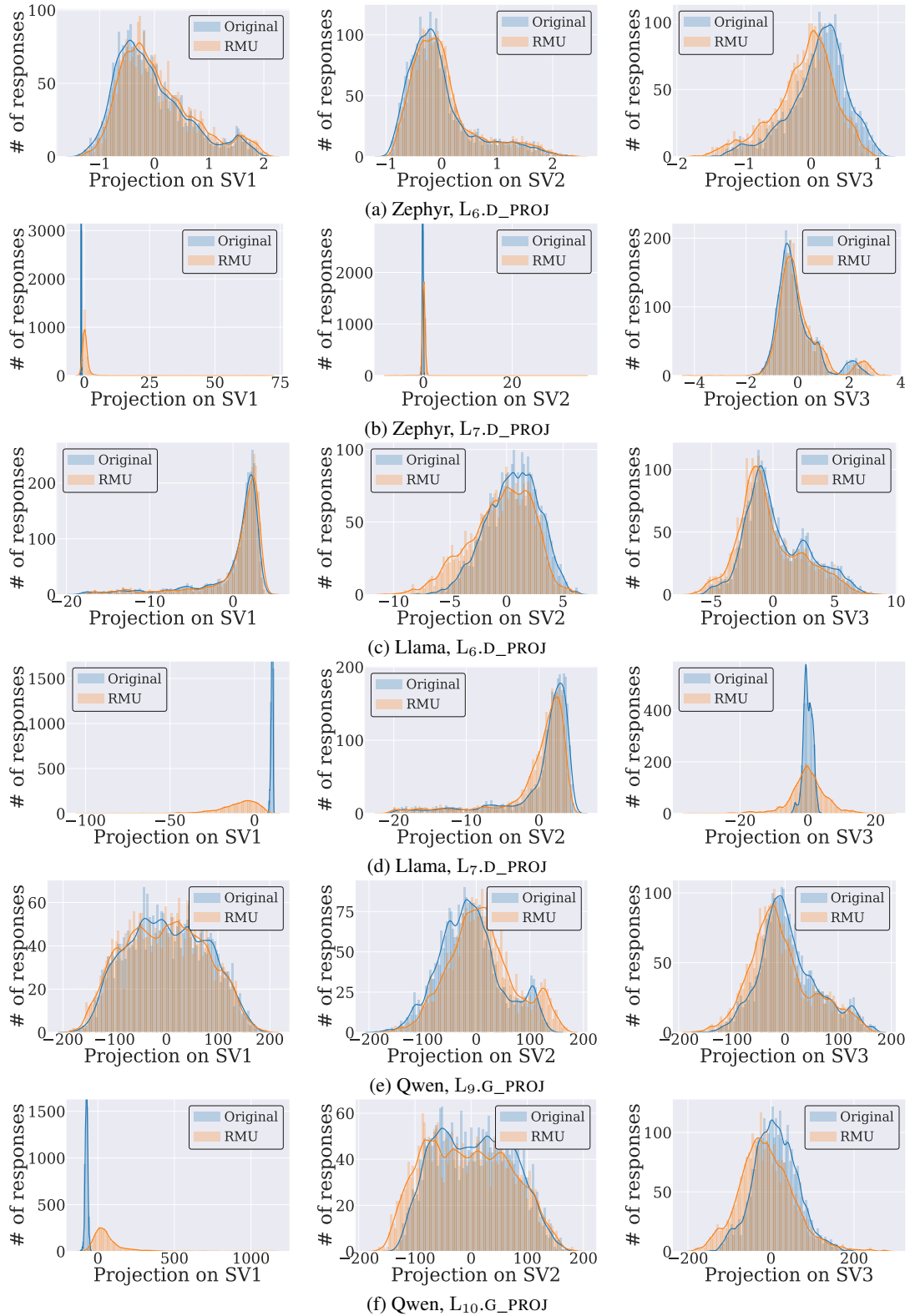


Figure A2: Projection of activations from various layers for 3000 responses to MMLU onto the three leading right singular vectors for the original and unlearned model. $L_i.D_PROJ$ refers to activations extracted from the down-projection sublayer of the FFN in the i -th transformer block, while $L_i.G_PROJ$ refers to activations extracted from the gate-projection sublayer of the FFN in the i -th transformer block (a,b) are projections for Zephyr-7B, (c,d) are for Llama3.1-8B, while (e,f) are for Qwen2.5-14B.

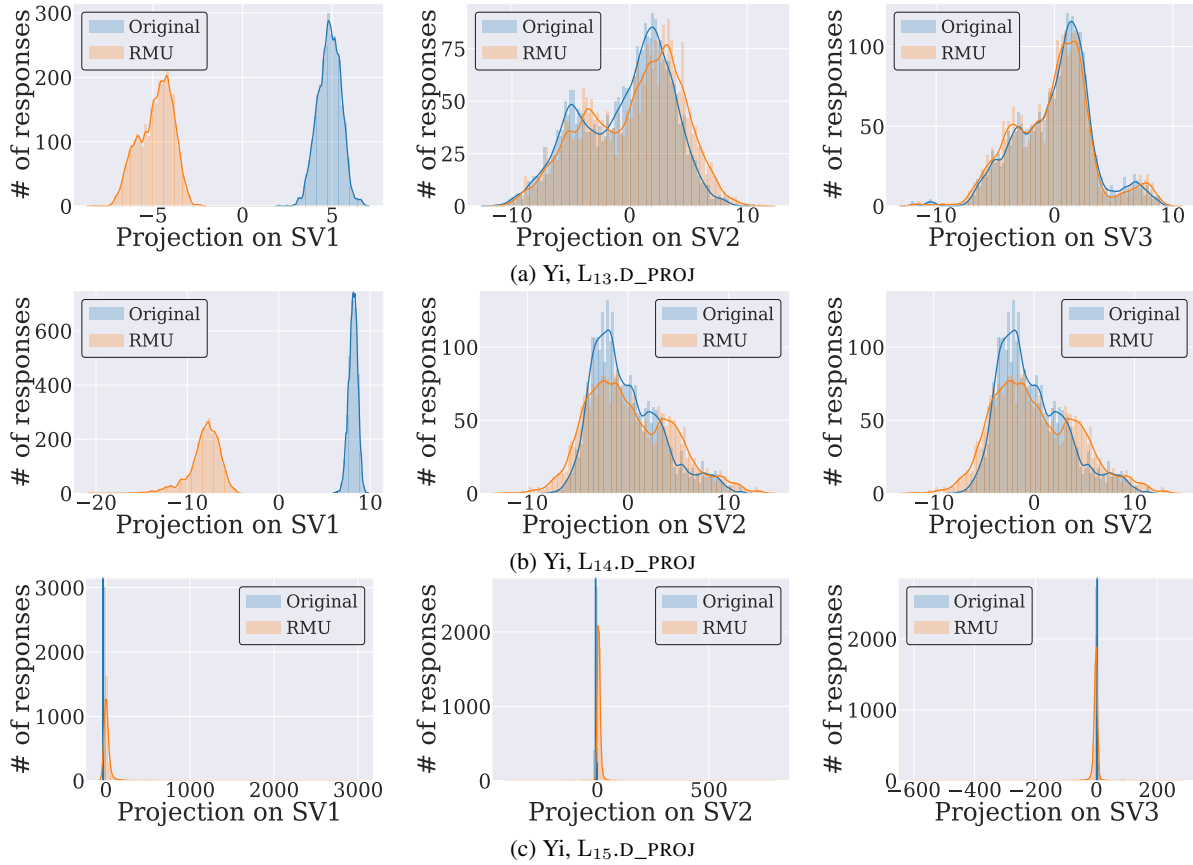


Figure A3: Projection of activations of Yi-34B-Chat from various layers for 3000 responses to MMLU onto the three leading right singular vectors for the original and unlearned model. $L_i.D_PROJ$ refers to activations extracted from the down-projection sublayer of the FFN in the i -th transformer block (a) are projections from layer 13, (b) are from layer 14, (c) are from layer 15.

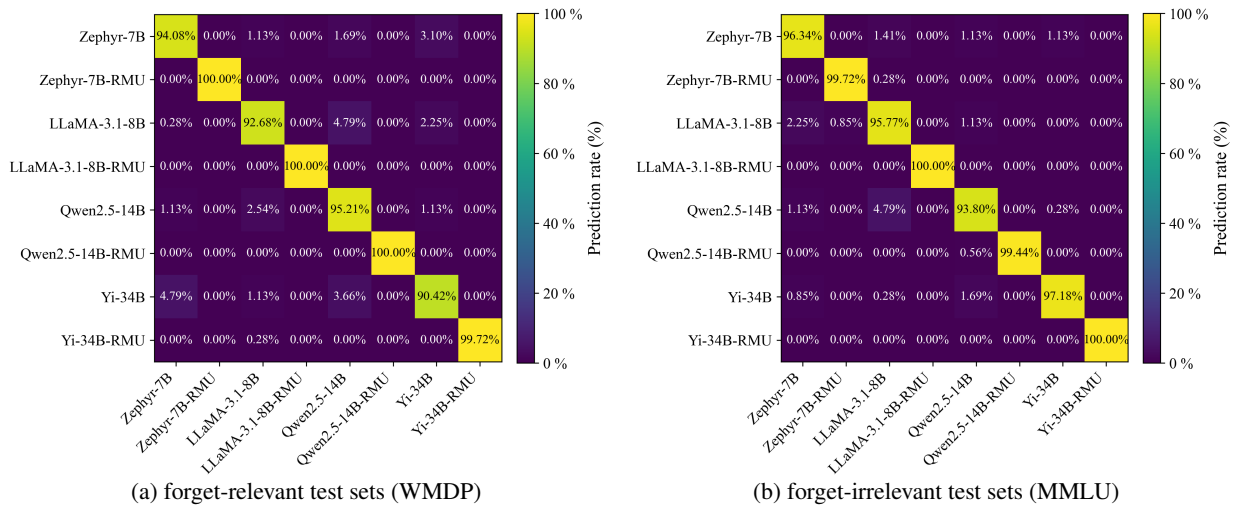


Figure A6: Confusion matrix for NPO-unlearning pair classification. Rows indicate true classes (original/NPO-unlearned model variants), and columns show predicted classes. Diagonal entries represent correct predictions; off-diagonals indicate misclassification rates under (a) WMDP and (b) MMLU test sets.